JOURNAL OF SOLID STATE CHEMISTRY 14, 219–228 (1975)

Crystal Structure of Vanadium Suboxide $V_2O_{1\pm x}$

KENJI HIRAGA AND MAKOTO HIRABAYASHI

The Research Institute for Iron, Steel and Other Metals, Tohoku University, Sendai, Japan

Received June 17, 1974; Received in Revised form August 25, 1974

A monoclinic structure with the unit cell content $2V_7O_3$ and its derivative structure designated as V_7O_{3+x} have been determined by X-ray and electron diffraction study. In both the structures, the oxygen atoms occupy regularly special octahedral interstitial sites in the body-centered monoclinic (or pseudo-tetragonal) metal lattice with the axial ratio $c/a \approx 1.2$. The ordered distribution of the oxygen atoms is interpreted from the condition of minimization of the elastic strain in the vanadium lattice.

Introduction

Recently much interest has been focused upon vanadium oxides in connection with metal–insulator transitions in V_nO_{2n-1} (*1*). However, the crystal structures and the phase relationships of vanadium suboxides with the composition $O/V \lesssim 1/2$ have not so far been established.

The present study is undertaken to determine the structure of the suboxide designated as $V_2O_{1\pm x}$ or γ phase existing below about 1100°C. Some contradictions have been noticed in previous reports on the crystal structure of this phase. According to an X-ray work of Westman (*2*), the V_2O phase has a monoclinic unit cell, of which the lattice constants are five times the three axes of the metal sublattice; $A = 5 \times 2.942$ Å, $B = 5 \times 2.926$ Å, $C = 5 \times 3.585$ Å and $\beta = 90.38°$ at $O/V = 0.53$. Cambini, Pellegrini, and Amelinckx (*3*) proposed a different monoclinic cell with $A = 9.52$ Å, $B = 2.95$ Å, $C = 7.77$ Å and $\beta = 90.66°$, which contains $2V_7O_4$ in seven cells of the metal sublattice, but did not determine the arrangement of oxygen atoms.

In the present paper, we propose a superstructure of the metal sublattice with ideal stoichiometry V_7O_3 in the hypostoichiometric region $O/V = 0.44$–0.48, and its derivative structure which will be denoted as V_7O_{3+x} in the hyperstoichiometric region $O/V = 0.52$–0.54. In these structures, the oxygen atoms are distributed regularly in special octahedral interstitial sites of the metal sublattice. The oxygen arrangements are discussed in terms of the elastic energy associated with the displacement of the nearest neighbor metal atoms, which is caused by the oxygen atoms situated in the octahedral interstitial sites of the metal sublattice.

Experimental Procedures

Several specimens in the concentration range $O/V = 0.44$–0.58 were prepared by the same method as in the previous work (*4*). The specimens were annealed at 1000°C for one week under vacuum and then cooled slowly to room temperature. The oxygen contents of the specimens were determined from the increase in weight on oxidation to form the pentaoxide V_2O_5 as the end product by heating in air at 650°C for one week, and agreed very well with the nominal compositions.

To prepare thin foils for electron diffraction and electron microscopy, bulk specimens were cut to 0.5 mm thick and the slices were jet-polished with use of a solution of 20% sulphuric acid and 80% methanol. The final thinning was done by a conventional electropolishing method with the same solution until a perforation was detected. X-ray powder diffractometry was made with filtered Cu$K\alpha$ radiation.

Experimental Results

Lattice parameters of the Metal Subcell

The metal subcell of the γ-$V_2O_{1\pm x}$ phase is monoclinic (or pseudotetragonal); $c > a \gtrsim b$,

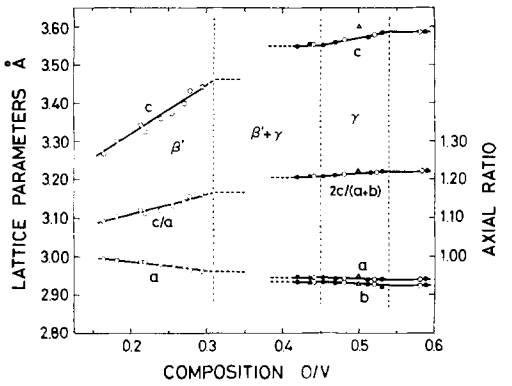

FIG. 1. Lattice parameters of the metal subcell of γ–$V_2O_{1\pm x}$ as a function of composition together with the values of β' phase (*4*). Data by Westman (*2*) and Cambini *et al.* (*3*) are plotted by full circles and triangles, respectively.

$c/a \approx 1.20$ and $\beta_0 \approx 90.3°$. In Fig. 1, the lattice parameters are plotted as a function of oxygen content together with those of the tetragonal β' phase (*4*), being in good agreement with the previous data (*2*, *3*). Since the data are lying approximately on an extrapolation of those of the β' phase, it is reasonable that the oxygen atoms in $V_2O_{1\pm x}$ occupy the octahedral interstitial sites between closest vanadium atoms along $[001]_m$ similarly to the case of the β' phase[1].

Electron Microscopic Observation

Prior to analyzing the crystal structure, microstructures were examined by transmission electron microscopy. An example of electron micrographs is shown in Fig. 2. We can see a number of antiphase boundaries roughly parallel to $[\bar{1}02]_m$, many of which are terminated at dislocations as was observed

[1] The index subscribed by *m* refers to the metal sublattice.

FIG. 2. A transmission electron micrograph of $VO_{0.48}$, showing a number of antiphase boundaries. The foil surface is nearly parallel to $(010)_m$.

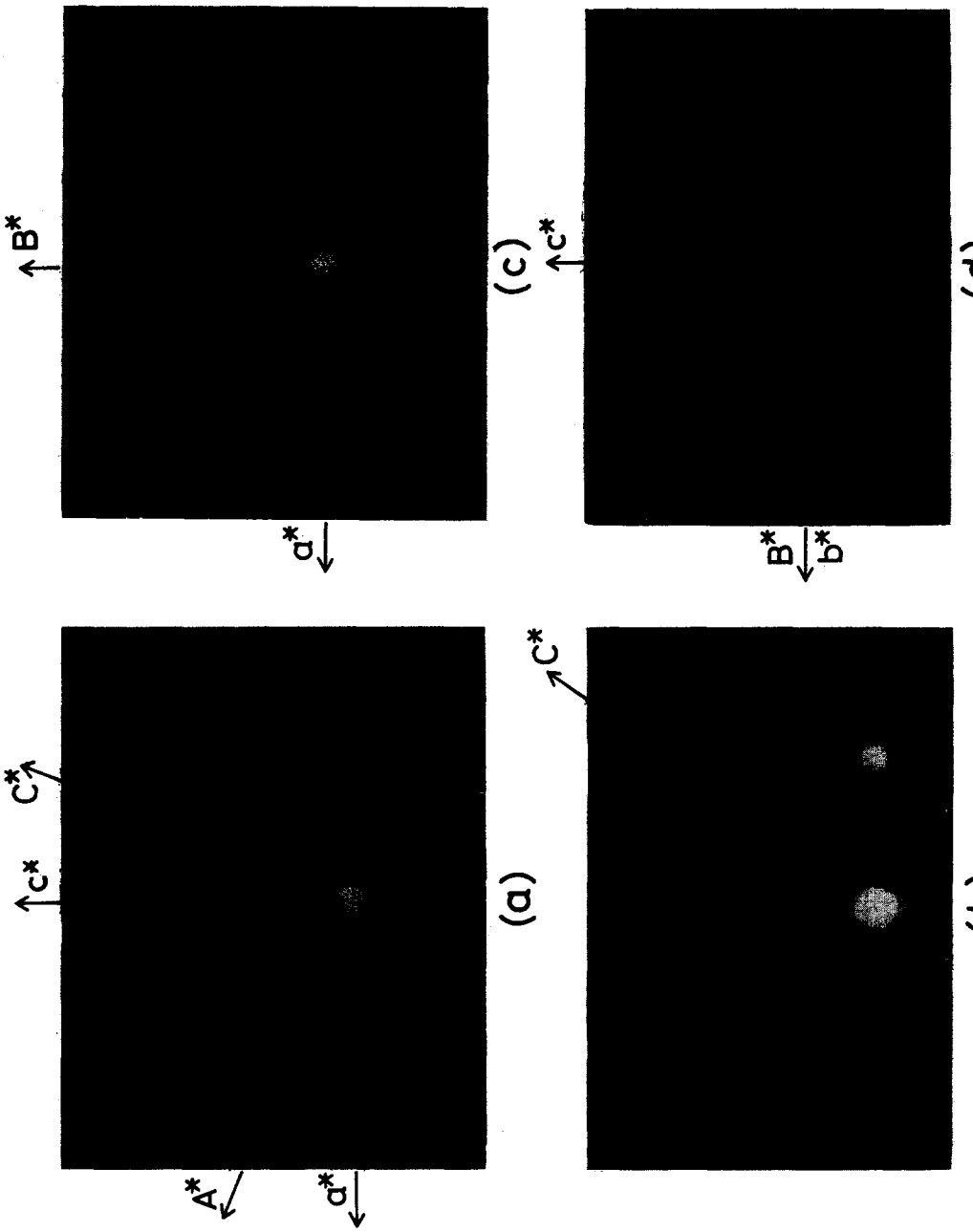

FIG. 3. Electron diffraction patterns of $VO_{0.44}$. Incident beam is parallel to $[010]_m$ in (a), $[311]_m$ in (b), $[001]_m$ in (c), and $[100]_m$ in (d).

by Cambini *et al.* (*3*). The microscopic observation suggests that the structure of $V_2O_{1\pm x}$ may have various kinds of displacement vectors with respect to the oxygen arrangement. This characteristic will become clear from the structure which will be presented in the following section.

Structure of V_7O_3

Some selected-area electron diffraction patterns of a specimen O/V = 0.44 are shown in Fig. 3, where the indices refer to the monoclinic metal lattice. In the patterns (*a*) and (*b*), in addition to strong fundamental reflections, a number of superlattice spots are lying parallel to the line connecting the origin and $\bar{1}03_m$ spot with the spacing of 1/7 of the distance between the two spots. However, no superlattice spot appears in the patterns (*c*) and (*d*), which correspond to the $[001]_m$ and $[100]_m$ incidences, respectively.

All the diffraction patterns observed agree with the constructed reciprocal lattice of Fig. 4, where large and small circles correspond to the fundamental and superlattice reflections, respectively. The result seems to be consistent with that of Cambini *et al.* (*3*), and gives the relations between the indices h, k, l for the fundamental lattice and those H, K, L for the superlattice, i.e., $H = 3h + l$, $K = k$ and $L = 2l - h$.

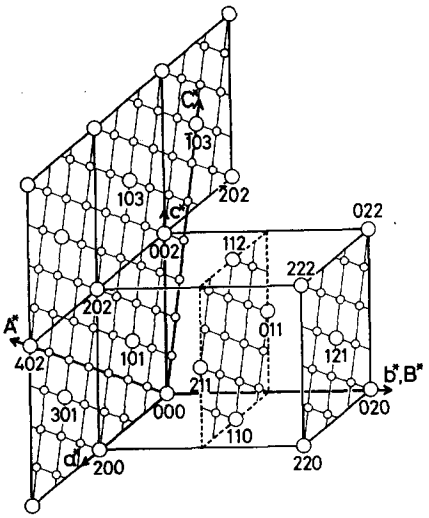

FIG. 4. Reciprocal lattice for the V_7O_3 structure. Large and small circles are the fundamental and superlattice reflections, respectively. Indices refer to the metal sublattice.

The diffraction patterns can be interpreted by a monoclinic cell with $A = (9a^2 + c^2 + 6ac\cdot\cos\beta_0)^{1/2} \simeq 9.5$ Å, $B = b \simeq 2.9$ Å, $C = (a^2 + 4c^2 - 4ac\cdot\cos\beta_0)^{1/2} \simeq 7.7$ Å and $\beta = 90.8°$, which is illustrated in Fig. 5(a). It is noted here that the cell dimension is identical with that proposed by Cambini *et al.* (*3*), but the direction of the vector **A** is opposite to that in their model.

The space group $C2/m$ is chosen to describe the structure, as deduced from the symmetry as well as from the observed extinction rule that no reflections appear for $H + K = 2n + 1$. The unit cell contains seven cells of the metal sublattice. It is quite reasonable, therefore, to assume the ideal stoichiometry $V_{14}O_6$ (O/V = 0.43) for this superstructure, taking into account the composition of the specimen O/V = 0.44. The atomic positions are then determined by comparing the observed patterns of electron diffraction as well as the intensity data of X-ray diffractometry with the calculated structure factors. The model is deduced from the following considerations.

1. All the oxygen atoms are on the octahedral interstitial sites between the closest metal atoms along $[001]_m$.
2. The vanadium atoms adjacent to the oxygen atoms are pushed apart from the ideal positions along $[001]_m$.

There are three possible sets of the oxygen distributions which satisfy the first condition, but the best agreement with the diffraction data can be obtained by the distribution listed in Table I. A projection of the atomic arrangement upon the $(010)_m$ plane is schematically illustrated in Fig. 5(b) by taking the area as large as $7a \times 7c$. It is seen from the figure that the oxygen atoms are lying on three successive planes parallel to $(\bar{1}03)_m$ and the oxygen atoms at the 4(*i*) sites are displaced slightly from the ideal octahedral positions along $[001]_m$ as indicated by arrows. The displacement is incorporated with that of the neighboring metal atom, and δ and δ' represent the displacements of the metal and oxygen atoms,

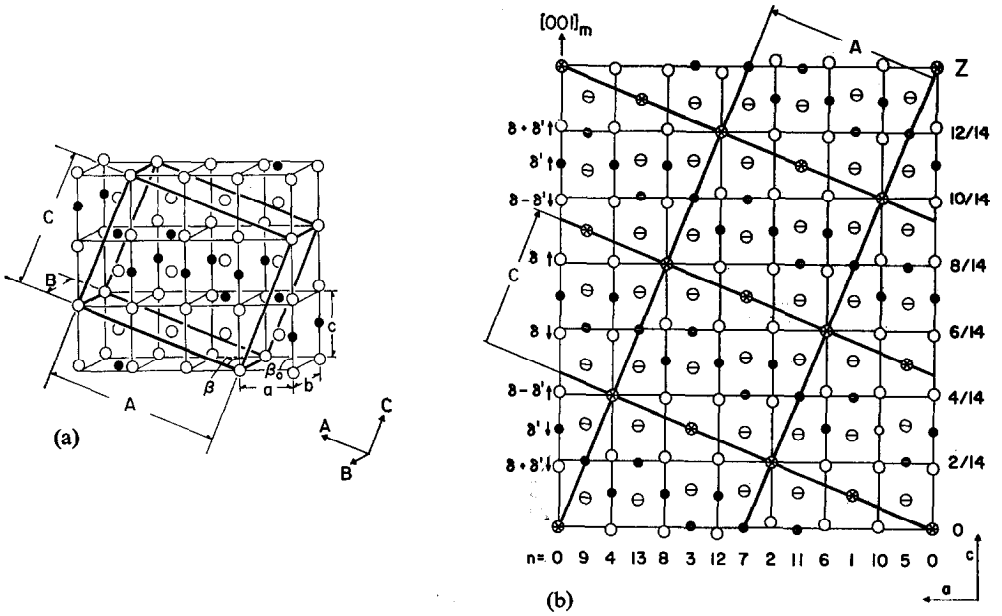

FIG. 5. (a) Monoclinic superstructure with stoichiometry V_7O_3. (b) Projection on $(010)_m$ plane of the large cell $7a \times 7c$. Open and full circles indicate vanadium and oxygen atoms, respectively. Circles with a horizontal bar represent the atoms lying on the plane $Y = 1/2$. Open circles with asterisks represent the metal atoms at the origins of the atomic rows parallel to $[001]_m$, of which the Z coordinate is given in terms of n of $Z = n/14$ in the bottom.

TABLE I

SUPERSTRUCTURE OF V_7O_3

Space group:	$C2/m$ (No. 12), monoclinic.
Unit cell dimension:	$A = (9a^2 + c^2 + 6ac\cdot\cos\beta_0)^{1/2} \simeq 9.5$ Å
	$B = b \simeq 2.9$ Å
	$C = (a^2 + 4c^2 - 4ac\cdot\cos\beta_0)^{1/2} \simeq 7.7$ Å
	$\beta = \cos^{-1}[(2c^2 - 3a^2 + 5ac\cdot\cos\beta_0)/AC] \simeq 90.8°$
Atomic position:	(0, 0, 0; 1/2, 1/2, 0) +
2 V in 2(*a*):	0, 0, 0.
2 O in 2(*d*):	0, 1/2, 1/2.
12 V in 4(*i*):	$x, 0, z; \bar{x}, 0, \bar{z}$
	$x = \{1 - (\delta + \delta')\}/7, z = 3\{1 - (\delta + \delta')\}/7$
	$x = (3 - \delta)/7, z = (2 - 3\delta)/7$
	$x = \{5 - (\delta - \delta')\}/7, z = \{1 - 3(\delta - \delta')\}/7.$
4 O in 4(*i*):	$x = (3 - 2\delta')/14, z = 3(3 - 2\delta')/14,$ where $\delta = 0.080$ and $\delta' = 0.014$.

being evaluated, respectively, as 0.080 ± 0.008 and 0.014 ± 0.005 from X-ray powder diffractometry.

As listed in Table II, the structure factors observed by X-ray diffractometry agree well with the results calculated from this model, being R factor ~0.15. The present model can also well explain the X-ray diffraction data obtained by the previous workers (*2*, *3*). An attempt was made to interpret the diffraction data in terms of other models which belong to space groups Cm and $C2$, but the present

TABLE II

COMPARISON OF THE LATTICE SPACINGS AND STRUCTURE FACTORS OF $VO_{0.44}$
($A = 9.507$ Å, $B = 2.935$ Å, $C = 7.695$ Å, $\beta = 90.84°$; $B = 1.2$ Å^2)

hkl	d_{obsd}	d_{calcd}	$\|F\|_{obsd}$	$\|F\|_{calcd}$	hkl	d_{obsd}	d_{calcd}	$\|F\|_{obsd}$	$\|F\|_{calcd}$
0 0 1	7.705	7.694	5	2	$\bar{1}$ 1 6	1.168	1 168	29	34
0 0 2	3.846	3.847	6	4	$\bar{4}$ 0 6	1.135	1.136	71	78[a]
$\bar{2}$ 0 2	3.01	3.012	6	12	$\bar{2}$ 2 4		1.135		
2 0 2		2.969			2 2 4	1.130	1.130		
1 1 1	2.634	2.630	4	5	8 0 2		1.130		
0 0 3	2.566	2.565	12	16	$\bar{3}$ 1 5	1.114	1.114	17	24
$\bar{2}$ 0 3	2.271	2.271	120	106	8 0 3	1.072	1.072	29	34
4 0 1	2.261	2.261			$\bar{6}$ 2 1	1.068	1.068	17	6
2 0 3	2.247	2.244			$\bar{6}$ 2 2	1.039	1.039	55	50
3 1 0	2.154	2.153	13	5	2 2 5	1.034	1.034	22	30
$\bar{3}$ 1 1	2.079	2.079	100	100	$\bar{4}$ 0 7	1.003	1.003	21	27
4 0 2	2.009	2.009	45	53	4 0 7	0.9920	0.9922	15	13
1 1 3	1.889	1.888	34	48	6 0 6	0.9898	0.9898	43	43
$\bar{2}$ 0 4	1.792	1.792	33	43	3 1 7	0.9754	0.9751	36	42
2 0 4	1.774	1.774	60	57	$\bar{9}$ 1 2	0.9654	0.9654	15	14
$\bar{3}$ 1 3	1.657	1.657	9	2	0 2 6		0.9656		
$\bar{1}$ 1 4	1.589	1.589	20	29	0 0 8	0.9618	0.9618	38	40
$\bar{6}$ 0 1	1.556	1.556	16	8	10 0 0	0.9505	0.9505	23	26
$\bar{6}$ 0 2	1.473	1.472	70	75	$\bar{8}$ 0 5	0.9472	0.9472	40	34
5 1 2	1.468	1.468	68	84[a]	1 3 2	0.9429	0.9430	32	31
0 2 0		1.467			6 2 4	0.9354	0.9355	19	12
2 0 5	1.458	1.458	39	44	$\bar{9}$ 1 3	0.9309	0.9309	42	42
$\bar{1}$ 1 5	1.352	1.352	43	46	$\bar{3}$ 3 1	0.9283	0.9283	41	42
5 1 3	1.347	1.347	38	41	9 1 3	0.9223	0.9224	16	11
0 0 6	1.282	1.282	13	17	8 2 1	0.9156	0.9156	20	16
$\bar{3}$ 1 5	1.257	1.258	8	8	1 3 3	0.9091	0.9093	26	21
3 1 5	1.246	1.246	19	17	$\bar{4}$ 2 6	0.8980	0.8980	31	28
$\bar{5}$ 1 4	1.232	1.232	121	112	8 2 2	0.8956	0.8956	23	22
$\bar{2}$ 2 3		1.232			7 1 6	0.8827	0.8828	17	13
7 1 0		1.232			$\bar{3}$ 1 8	0.8816	0.8814		
2 2 3	1.227	1.228			0 2 7	0.8799	0.8798		
5 1 4	1.221	1.221	34	38	$\bar{1}$ 3 4	0.8687	0.8688	13	13
7 1 1	1.214	1.214	32	35	8 2 3	0.8657	0.8657	26	25
4 2 2	1.184	1.185	23	32					

[a] A comparison of $(I/Lp)^{1/2}$ is made in place of the structure factor, where I and Lp are the intensity and the Lorentz-polarization factor, respectively.

model appears to give the best agreement with the data.

An important feature of the large V_7O_3 cell shown in Fig. 5(b) is that every atomic row parallel to $[001]_m$ consists of seven vanadium atoms and three oxygen atoms with the same sequence V*·VOV·VOV·VOV·, where · indicates the vacant octahedral site. In these sequences, the three oxygen atoms are distributed evenly in the seven interstitial sites so as to minimize the lattice strain in the atomic row. In other words, this is a unique structure in which the oxygen atoms do not occupy two successive octahedral interstitial sites in such a way as ·VOVOV·. The configuration of these atomic rows in the lateral direction normal to $[001]_m$ will be discussed later. For the sake of convenience for the discussion, the coordinate of each row along $[001]_m$ is given in terms of $Z = n/14$, that is the coordinate of

the metal atom marked with an asterisk, and n (=0 to 13) is given in the bottom of Fig. 5(b).

It is seen from this model that antiphase boundaries with respect to the oxygen distribution would be possible to form easily with various kinds of out-of-step vectors.

Structure of V_7O_{3+x}

Typical electron diffraction patterns of a specimen O/V = 0.52 are shown in Fig. 6 with schematical illustrations. In addition to the reflections of the V_7O_3 structure, we can see many extra reflections which are indexed as $2n$ $(4n \pm 1)/2 \pm \varepsilon$ $(2n+1)/2$ and $2n+1$ $(4n \pm 1)/2 \mp \varepsilon$ $(2n+1)/2$ in terms of the V_7O_3 structure. The zigzag distribution of the extra reflections in Fig. 6(b) is also interpreted in terms of the fractional parameter ε.

The reciprocal lattice depicted in Fig. 7 is constructed by a similar process to the case of the V_7O_3 structure. This is characterized by the appearance of paired extra reciprocal planes with $K = 1/2 \pm \varepsilon$, $3/2 \pm \varepsilon \ldots$, on which the extra superlattice reflections are lying as shown in Fig. 7. If we neglect the parameter ε, the indices for the extra reflections are given by $H' = H$, $K' = 2K$ and $L' = 2L$ in terms of the indices for the V_7O_3 structure, and the systematic absence of reflections is expressed as $K' + L' = 2n + 1$. These extra reflections are considerably broadened along the A^* axis, and a reason for this broadening will be discussed later briefly.

The value of ε is so small (~0.01) that the new superlattice is primarily considered to have the cell dimension $A \times 2B \times 2C$. Based

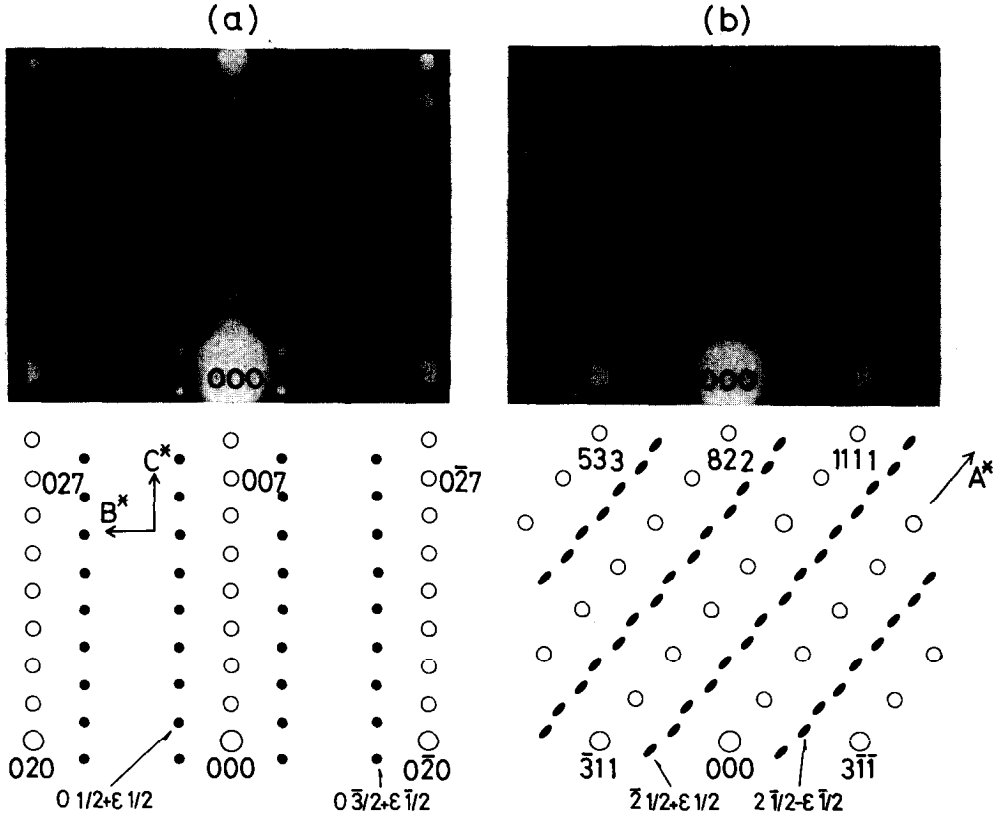

FIG. 6. Electron diffraction patterns of $VO_{0.52}$. Incident beam is parallel to $[301]_m$ in (a) and $[11\bar{2}]_m$ in (b), which correspond to [100] and $[0\bar{1}1]$ of the V_7O_3 superlattice, respectively. Indices given in the patterns and in the illustrations refer to the metal sublattice and the V_7O_3 superlattice, respectively. Full circles indicate the extra superlattice reflections for V_7O_{3+x}.

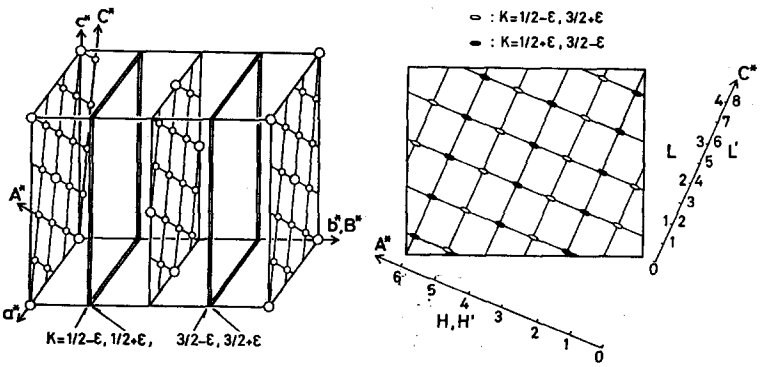

FIG. 7. Reciprocal lattice for the V_7O_{3+x} structure. In addition to the reflections of the V_7O_3 structure located on the *HL* planes with $K = 0, 1, 2, \ldots$, the extra reflections appear on the paired *HL* planes with $K = 1/2 \pm \varepsilon$, $3/2 \pm \varepsilon$ and so on.

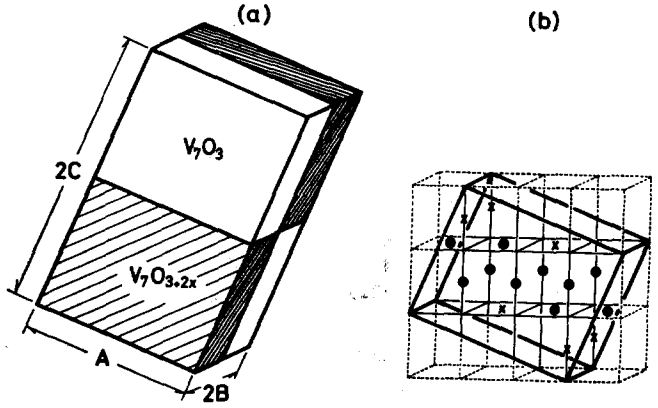

FIG. 8. (a) A basic model of the V_7O_{3+x} structure composed of the V_7O_3 and V_7O_{3+2x} subcells. (b) Oxygen distribution in the V_7O_{3+2x} subcell. Excess oxygen atoms occupy statistically the interstitial sites marked by crosses with the occupation probability x.

on the observed extinction rule $K' + L' = 2n + 1$, we can deduce a basic model of V_7O_{3+x} in which two kinds of subcells with the dimension $A \times B \times C$ are paired in both the directions of the vectors **B** and **C** as schematically depicted in Fig. 8: one of the subcells is the V_7O_3 cell and another one containing excess oxygen atoms is denoted as V_7O_{3+2x}.

For this model, the structure factors for the extra reflections (K' and $L' =$ odd) are given as the difference between those for the two kinds of the subcells. The observed intensity of these reflections were so weak in comparison with the superlattice reflections (K' and $L' =$ even) for the V_7O_3 structure that the distribution of the excess oxygen atoms could not be definitely determined from quantitative comparison of the observed and calculated structure factors. However, we can propose a most probable distribution of the excess oxygen atoms, which is presented in Fig. 8(b), from a consideration on lattice strain owing to the oxygen distribution. In the above mentioned atomic rows parallel to $[001]_m$ in the V_7O_3 structure (Fig. 5(b)), two octahedral sites in both sides of the vanadium atom at the origin remain unoccupied in pair (V·V*·V), while other vacant sites are not paired (V·VO or OV·V). Therefore, the excess oxygen atoms prefer to occupy statistically the former, which corresponds to the 4(*i*) positions with $x \simeq 1/14$ and $z \simeq 3/14$, rather than the others so as to minimize the lattice strain. When these sites are completely filled, the composition

of the large superlattice becomes V_7O_4 (O/V = 0.52), being very close to the limit of the homogeneity range of the γ phase.

The crystal structure of O/V $\gtrsim$ 0.5 is primarily based on the above model, but it may be modified by taking account of $\varepsilon \neq 0$. From the analogy of nonintegral periods of antiphase domain structures in binary substitutional alloys (*8*), the fractional parameter ε is attributed to the fact that the period along [010] of the V_7O_{3+x} structure is slightly less than $2B$ by a random mixing of the regions with the period B in the matrix. The existence probability of the region with the period B is estimated as about 1/20 from the observed value of ε.

It is suggested further that out-of-steps with respect to the distribution of the excess oxygen atoms take place approximately normal to [100] in the V_7O_{3+x} structure. The anisotropic size effect of the antiphase domains may be the reason for the broadening of the extra reflections along the A^* axis. It is likely to grow such domains during the ordering process of the oxygen atoms.

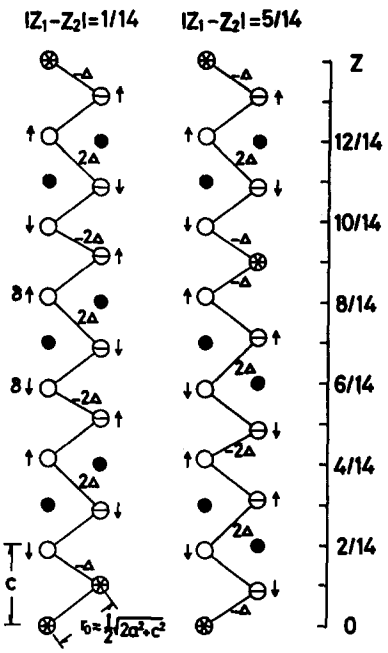

FIG. 9. Combinations of the parallel atomic rows with $|Z_1 - Z_2| = 1/14$ and 5/14. For simplicity, the interatomic distances $r_0 \pm \Delta$ and $r_0 \pm 2\Delta$ are denoted as $\pm\Delta$ and $\pm 2\Delta$, respectively.

Discussion and Conclusion

The V_7O_3 structure and its derivative V_7O_{3+x} structure belong to the same family as those of α'–V_8O (or V_9O) (*5–7*) and β'–$V_{16}O_3$ (*4*), since the oxygen atoms in these structures are distributed regularly in the octahedral interstitial sites in the host metal lattice. The radius of the oxygen atoms situated in the V_7O_3 structure is estimated as about 0.76 Å, which is somewhat longer than the covalent radius (0.66 Å). The two metal atoms are displaced along $[001]_m$ by $\delta c \approx 0.28 \pm 0.03$ Å, which is nearly equal to that (0.27 Å) in the $V_{16}O_3$ structure (*4*).

We will discuss the elastic energy associated with the displacement of the nearest neighbor metal atoms. Since the sequences of the atomic arrangement parallel to $[001]_m$ are identical in every atomic row in the V_7O_3 structure, the elastic energy varies with configurations of the neighboring atomic rows in the lateral direction. For examples, Fig. 9 shows the pairs of the parallel rows with the coordinates Z_1 and Z_2; $|Z_1 - Z_2| = 1/14$ and 5/14. There are five kinds of the interatomic distances r_0, $r_0 \pm \Delta$ and $r_0 \pm 2\Delta$ between the nearest neighbor metal atoms, where $r_0 \approx (2a^2 + c^2)^{1/2}/2 \approx 2.74$ Å and $\Delta = \delta c \cdot \cos\tau \approx 0.18$ Å [$\tau \approx \tan^{-1}((2a)^{1/2}/c)$], neglecting the parameter δ'. If we denote the numbers of the nearest neighbor pairs with the interatomic distances r_0, $r_0 \pm \Delta$ and $r_0 \pm 2\Delta$ as N_0, N_1 and N_2 respectively, the strain energy associated with the displacements $\pm\Delta$ and $\pm 2\Delta$ is proportional to $(N_1 + 4N_2)\Delta^2$. For all combinations of the paired atomic rows, the values $N_1 + 4N_2$ are listed in Table III. We can see that the strain energy is minimum for the paired rows with $|Z_1 - Z_2| = 5/14$.

It turns out from Fig. 5 that the V_7O_3 structure actually consists of these combinations; the oxygen atoms are distributed so as to minimize the elastic energy for the given oxygen concentration. The location of excess oxygen atoms in the V_7O_{3+x} structure may also be understood from the same point of view. One can conclude, therefore, that the short range field of elastic strain caused by

TABLE III

NEAREST NEIGHBOR PAIRS OF THE METAL ATOMS

Difference in the Z coordinates of the paired rows $\lvert Z_1 - Z_2 \rvert$	Number of the metal atom pairs N_0	N_1	N_2	$N_1 + 4N_2$
1/14	7	2	5	22
3/14	4	4	6	28
5/14	6	4	4	20
7/14	4	4	6	28

the interstitial oxygen atoms plays an essential role in the structure of γ-$V_2O_{1\pm x}$.

Acknowledgments

This work was partly supported by the fund in Aid of Scientific Research by the Ministry of Education and by the Toray Science and Technology Grant. The support is gratefully acknowledged.

References

1. S. KACHI, K. KOSUGE, AND H. OKINAKA, *J. Solid State Chem.* **6**, 258 (1973).
2. S. WESTMAN, *Acta Chem. Scand.* **17**, 749 (1963).
3. M. CAMBINI, G. PELLEGRINI, AND S. AMELINCKX, *Mater. Res. Bull.* **6**, 791 (1971).
4. K. HIRAGA AND M. HIRABAYASHI, *J. Phys. Soc. Japan* **34**, 965 (1973).
5. M. CAMBINI, M. HEERSCHAP, AND R. GEVERS, *Mater Res. Bull.* **4**, 633 (1969).
6. M. HIRABAYASHI, S. YAMAGUCHI, K. HIRAGA, AND H. ASANO, *Proc. Intern. Conf. on Order-Disorder Transformations in Alloys*, 266, Tübingen (1973).
7. D. GUNWALDSEN AND D. POTTER, *J. Less-Common Metals* **34**, 97 (1974).
8. K. FUJIWARA, *J. Phys. Soc. Japan* **12**, 7 (1957).